Unsteady Aerodynamic Characteristics of an Accelerating or Decelerating Aerofoil

Y. -K. Lee and H. -D. Kim
School of Mechanical Engineering, Andong National University
Songcheon-Dong 388, Andong, Kyeongbuk, 760-749, Korea
Email: kimhd@andong.ac.kr

Keywords: Acceleration, Aerofoil, Deceleration, Subsonic Flow, Unsteady Aerodynamics

Abstract

The unsteady aerodynamic characteristics of an aerofoil gradually accelerating or decelerating at subsonic speeds are investigated through two-dimensional, unsteady, compressible Navier-Stokes simulations. An acceleration factor is defined to provide various acceleration or deceleration characters of the time-dependent flow over the aerofoil. The results show that an increase in the absolute value of the non-dimensional acceleration factor leads to a lesser change in the location and range of flow featues such as shockwave and boundary layer separation in a specific time range. Generally, the gradual speed-up and speed-down of the subsonic aerofoil results in different aerodynamic characteristics whose changes are more significant at angles of attack.

Introduction

Wing aerodynamics has been one of the most classical and popular research areas due to a variety of its applications such as aircraft[1], missiles[2], helicopters[3] and turbomachinery[4]. The flow physics basically issued at steady states have been well understood for subsonic to supersonic flight/operating conditions owing to the considerable efforts made through a number of experimental and numerical studies for many decades. Nonetheless, unsteady flow features and shock-boundary layer interaction occurring in the flowfield over aerofoils and associated phenomena such as dynamic stall[5], buffeting[6] and hysteresis behaviors[7] at high angles of attack are not fully understood yet.

In flight, flow unsteadiness is inevitably existent at any flight conditions due to mainly two different reasons, say, time-dependent disturbances or self-generated and self-sustained flow instabilities. Regarding the former reason, especially, an abrupt change in the flight speed can be an important source of external disturbances and it has been much known through past investigations[8]. The unsteadiness due to a gradual speed change at subsonic speeds, meanwhile, has not been investigated to date to the authors' knowledge even though it can happen generally for any aircraft.

Flight bodies experience gradually accelerating or decelerating flows essentially at take-off and landing with angles of attack. Especially, when a shockwave is onset on an aerofoil, even a slight speed change can lead to a significant variation in SBLI (shock-boundary layer interaction) features, which are generically unsteady and have strong instability. Thus this type of speed-up or speed-down can introduce a continuous and irregular change in the SBLI features and associated wake flow in the boundary layer separation. In this situation, it is expected that the aerodynamic characteristics of aerofoils can depend on the history of the speed change.

In this study, unsteady aerodynamic characteristics of an aerofoil, NACA0012, accelerating or decelerating at subsonic speeds were numerically investigated. The present CFD (computational fluid dynamics) analysis was carried out using two-dimensional, unsteady compressible mass-averaged Navier-Stokes equations with the Spalart-Allmaras[9] turbulence model, discretized by a fully implicit finite volume scheme and a multi-stage Runge-Kutta method.

Numerical Simulations

Governing Equations

The present study adopted a commercial computational code, FLUENT 5, in order to analyze the unsteady aerodynamic characteristics of a subsonic aerofoil under a gradual speed change at zero angle of attack or angles of attack. Two-dimensional, unsteady mass-averaged Navier-Stokes equations governing the flowfield around a NACA0012 aerofoil were discretized by an implicit finite volume scheme spatially and a 4-stage Runge-Kutta time stepping scheme temporally.

The Spalart-Allmaras turbulence model was employed to close the governing equations. The turbulence model is a one-equation model recently developed, basically, for aerodynamic applications.[9] According to past studies[10] using this model, it can give good results not only for the prediction of adverse pressure gradients inside boundary layers but also for various unsteady problems issued in wing aerodynamics.

Grid System and Analysis

Fig. 1 shows the grid layouts of a C-typed computational domain and the near-field of the

NACA0012 profile used in the present study. About 15,000 nodes were applied to the computational domain, in which grids were clustered in the regions near wing surfaces in order to provide accurate predictions of shock-induced flow separation. The computational domain were set up with dimensions of 20 times of the chord c towards the upstream from the leading edge and 25 times of c towards the downstream from the trailing edge to meet free stream conditions and to obtain better convergence.

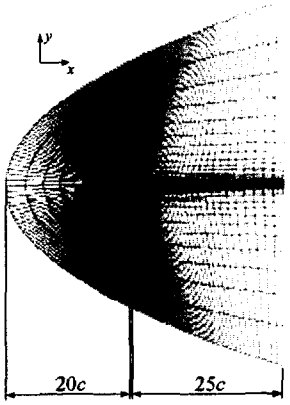

(a) Computational domain

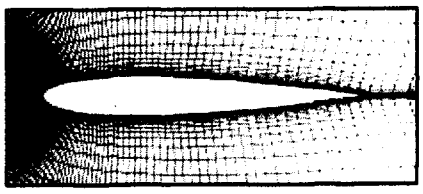

(b) Grid layout near the aerofoil model

Fig. 1 Two-dimensional structured grid system for NACA0012

The far-field boundary condition was applied to external boundaries of the computational domain. The free stream velocity U_∞ changes from 100 m/s to 300 m/s and from 300 m/s to 100 m/s, which are a gradual time-dependent speed-up (constant acceleration) and speed-down (constant deceleration) respectively. For simplicity, a constant pressure of 101325 Pa and a constant temperature of 300 K were used for the free stream boundaries.

To give different acceleration or deceleration characteristics of the aerofoil, a non-dimensional acceleration factor β was defined as follows:

$$\beta = \frac{(U_f - U_i)/T}{U_m / T_c} \qquad (1)$$

where U_f, U_i and U_m are the final, initial and mean velocities respectively. T is time needed for the acceleration from U_i to U_f, and T_c is time required for a flow particle with U_m to pass through the characteristic length of the aerofoil. As shown in Fig. 2, six values of β were tested at angles of attack of 0° ~ 10°.

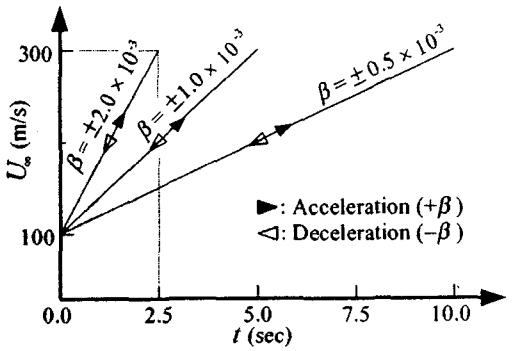

Fig. 2 Non-dimensional acceleration factor

Unsteady solutions were initialized from one of the steady state solutions obtained at U_∞ = 100 m/s (acceleration) and 300 m/s (deceleration). The solutions were considered converged when these satisfied the convergence criteria that the residuals of all equations were less than 1.0×10^{-4} and drag convergence ΔC_D was less than 1.0×10^{-7}. Time step sizes of 0.5×10^{-3} ~ 1.0×10^{-3} sec were selected in consideration of proper convergence satisfying the above criteria within 30 iterations for each time step. From the preliminary tests with several time step sizes, it has been found that a change in the drag coefficient C_D is negligible when a time step size is less than 1.0×10^{-3} sec.

Results and Discussion

The Mach number contours at α = 0° given in Fig.3 show the effect of accelerating time on the flowfield near the aerofoil model. The figures were selected for several representative conditions including strong shock-boundary layer interaction. As the aerofoil accelerates, typically, local supersonic regions increase and a shockwave suddenly occurs near the maximum thickness of the aerofoil. The shock moves rapidly towards the trailing edge with further increases in U_∞ and, consequently, the boundary layer behind the shock is separated (U_∞ = 300 m/s) by strong adverse pressure gradients there. With larger β, the generation of the shock and its rearward movement are retarded. At $\beta = 2.0\times10^{-3}$ and U_∞ = 300 m/s, shock-induced separation is apparently weak when compared with the steady state (β = 0).

Fig. 4 shows surface pressure distributions, given as the pressure coefficient C_p, with time for β = 0.5×10^{-3}, 1.0×10^{-3} and 2.0×10^{-3} (corresponding acceleration a = 20 m/s^2, 40 m/s^2 and 80 m/s^2 respectively). The pressure coefficients given in the figures are presented only for the suction side because the NACA0012 profile is exactly symmetric, resulting

in basically same distributions on both sides. Surface pressure decreases from the leading edge up to about 14 % chord (the maximum thickness is at about 30 % chord) and then increases along the curved surface with a thickened boundary layer. As long as the entire flowfield is subsonic, the location of the minimum pressure is nearly fixed at about x/c = 0.14. When a local supersonic region occurs at high subsonic speeds after 0.8 U_f, however, local acceleration along the curved surface is continued up to the presence of a sudden rise in pressure due to a shockwave. For all β, a similar trend of time-dependent C_p distributions is observed but shock generation and movement are shown to be relatively abrupt at lower β.

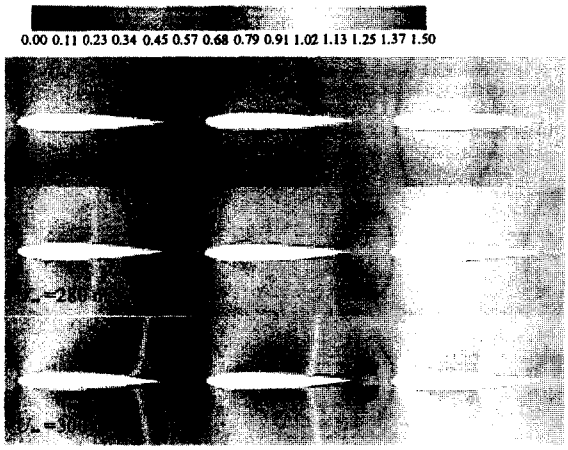

(a) $\beta = 0$ (steady) (b) $\beta = 1.0\times10^{-3}$ (c) $\beta = 2.0\times10^{-3}$

Fig. 3 Mach number contours for several β at acceleration and $\alpha = 0°$

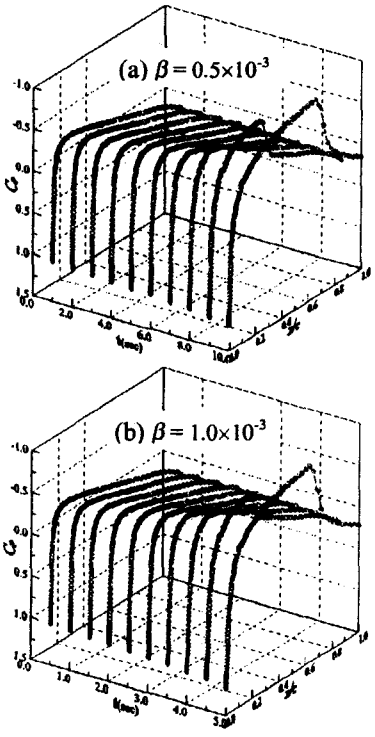

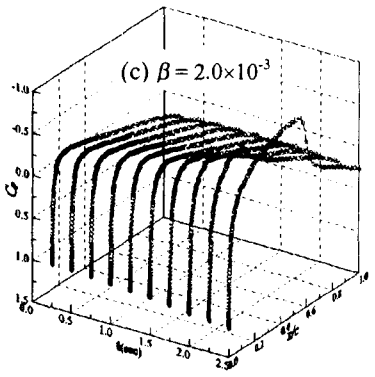

Fig. 4 Surface pressure distributions for several β at acceleration and $\alpha = 0°$

Fig. 5 shows the Mach number contours obtained for β = 0, 1.0×10^{-3} and 2.0×10^{-3} at an angle of attack of 10°. At the given α, a local supersonic flow with a shockwave occurs considerably earlier compared with the cases at zero angle of attack. It is observed that even a weak shockwave can induce large boundary layer separation on the suction side (U_∞ = 250 m/s) and further acceleration leads to a rearward shock movement with reduced separation on the aerofoil. The effect of β on shock generation and movement is found to be similar to the cases at zero angle of attack but more noticeable particularly at a high speed of 300 m/s.

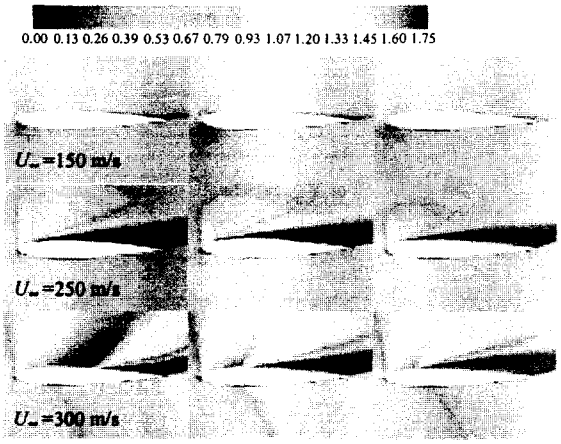

(a) $\beta = 0$ (steady) (b) $\beta = 1.0\times10^{-3}$ (c) $\beta = 2.0\times10^{-3}$

Fig. 5 Mach number contours for several β at acceleration and $\alpha = 10°$

At β = 0.5 × 10^{-3}, the pressure distributions shown in Fig. 6 present the influence of angle of attack on accelerating flow over the aerofoil. For a low angle of attack of 2°, the change in local C_p values with time shows similar aerodynamic characteristics to the values at $\alpha = 0°$ on both sides. At relatively high angles of attack, 5° and 10°, C_p distributions show opposite profiles between both sides without a shockwave while follow the similar

chordwise variations as those at zero angle of attack with a shockwave. It is interesting to note that the minimum C_p value and maximum shock strength are observed when the shock begins to occur. At higher angles of attack, as the shock is generated earlier, the shock on the suction side reaches its maximum strength more quickly. Then the shock becomes weaker with rearward movements during further acceleration.

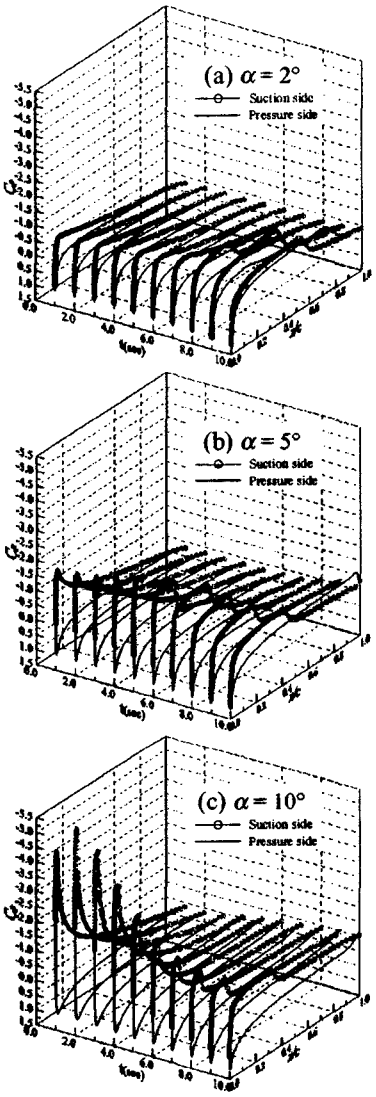

Fig. 6 Surface pressure distributions at angles of attack and $\beta = 0.5 \times 10^{-3}$

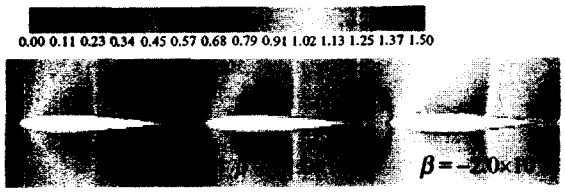

(a) $\alpha = 0°$ and $U_\infty = 280$ m/s

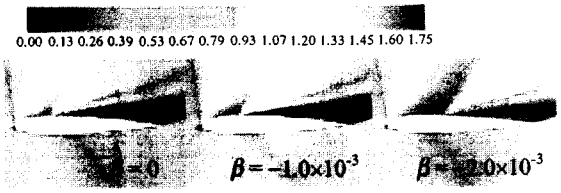

(b) $\alpha = 10°$ and $U_\infty = 280$ m/s

Fig. 7 Mach number contours at deceleration

Fig.7 show Mach number contours obtained at $U_\infty = 280$ m/s during deceleration. In both figures at α = 0° and10°, it can be observed that, generally, the upstream movement of the shock and separation can be retarded by increasing absolute β. However, the variation occurs less severely compared with those at acceleration.

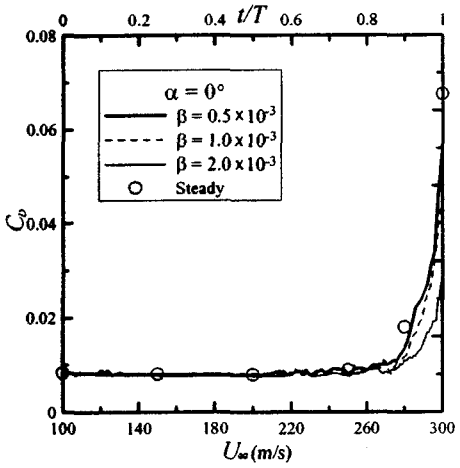

(a) Acceleration

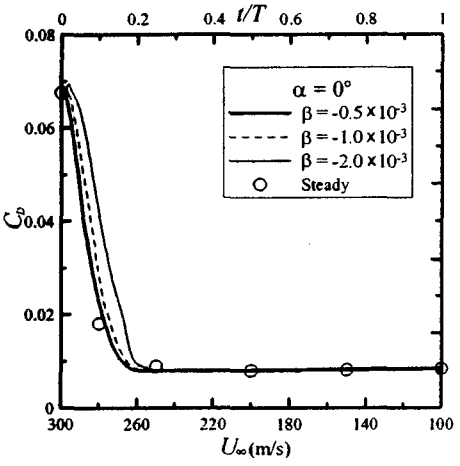

(b) Deceleration

Fig. 8 Drag histories at $\alpha = 0°$

Fig. 8 shows time-dependent drag histories given

by C_D values at zero angle of attack during acceleration and deceleration. The C_L variations for NACA0012 at zero angle of attack are insignificant due to the symmetry of the model so that a C_L history is not given in this figure.

In Fig. 8(a), C_D at first remains nearly constant if the entire flowfield is subsonic. Then it is fluctuating as a local supersonic region increases during acceleration and suddenly rises in the presence of a shockwave. With an increase in β, C_D values become lower due to a weaker shock-boundary layer interaction at a given time step as aforementioned with the previous figures (Fig. 3 and Fig.4). However, the C_D fluctuations shown at acceleration are not observed at deceleration (Fig. 8(b)). In addition, a lesser upstream movement of the shock and separation with an increased absolute β leads to larger drag in a specific t/T range. At deceleration, such a sudden change in drag is starts to occur at a higher speed.

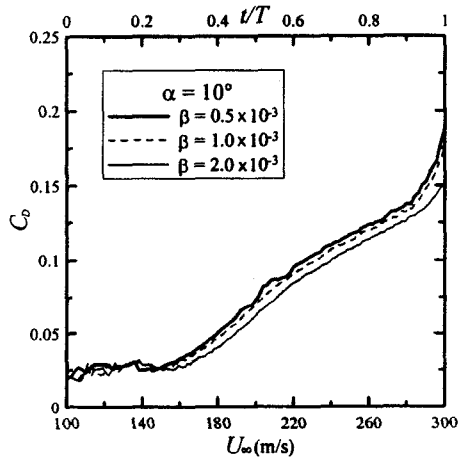

(a) Acceleration

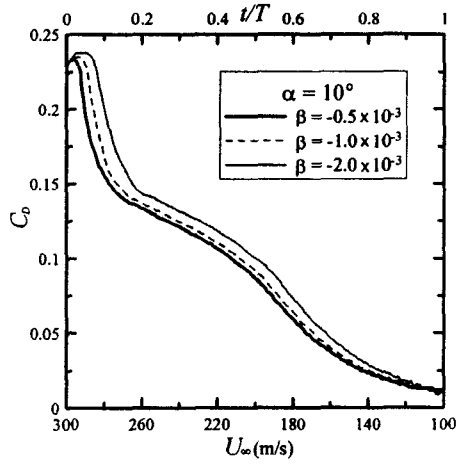

(b) Deceleration

Fig. 9 Drag histories at $\alpha = 10°$

At a high angle of attack of 10°, for acceleration (Fig. 9(a)), the aerodynamic characteristics presented in Fig. 8(a) can be also observed. But the fluctuations are present from the beginning of acceleration since a local supersonic region exists from a relatively lower speed. As the shockwave occurs from a speed of about 150 m/s, a reduction of C_D with an increased β is shown in a wide range of time t/T.

During deceleration (Fig. 9(b)), C_D fluctuations at low speeds are insignificant like the cases at zero angle of attack. However, drag is dependent on β in almost entire speed range tested. In this situation, at a given speed, drag becomes larger as absolute β increases.

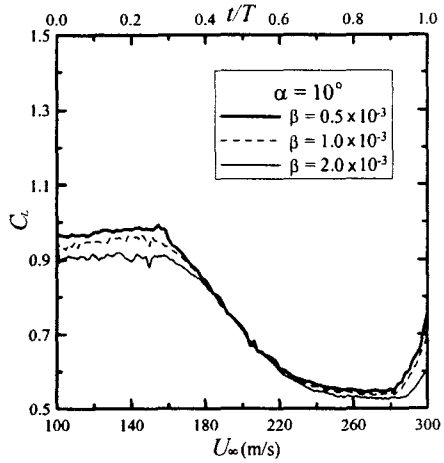

(a) Acceleration

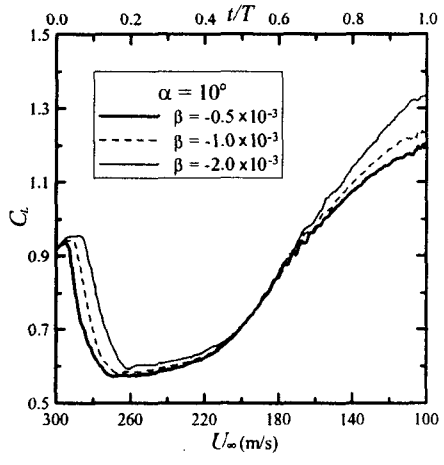

(b) Deceleration

Fig. 10 Lift histories at $\alpha = 10°$

At $\alpha = 10°$, Fig. 10 shows the lift histories during acceleration and deceleration. A fluctuating time-dependent C_L variation in a small range is observed up to a low speed of about 150 m/s at acceleration but it does not occur at deceleration. For the tested speed

range, ΔC_L at deceleration is larger about 44 % than the value at acceleration.

From the figures regarding drag and lift, it has been found that the aerodynamic characteristics of an aerofoil can be significantly changed depending on β values. In this study, the acceleration and deceleration is not simulated continuously. But the apparently different histories of the time-dependent changes in the subsonic aerofoil flowfields investigated imply that a hysteresis phenomenon can be occurred during a gradual speed change. Therefore, it is understood that the control of flight bodies at take-off or at landing must be conducted in consideration of the particular aerodynamic characteristics for a given accelerating or decelerating time and speed range.

Conclusions

The unsteady aerodynamic characteristics of a NACA0012 aerofoil under a gradual speed change at angles of attack as well as at zero angle of attack were investigated through two-dimensional Navier-Stokes computations. To obtain various accelerating and decelerating characters in a subsonic speed range, a non-dimensional acceleration factor was defined.

The results obtained from the present study showed that an increase in the non-dimensional acceleration factor led to lesser changes in the location and range of a shockwave and boundary layer separation on the aerofoil in a specific time range. Especially, the effect of the acceleration factor on aerodynamic characteristics was, in general, more significant at angles of attack during acceleration or deceleration. The time-dependent histories of drag or life were, however, apparently dissimilar for a given absolute value of the acceleration factor. It has been understood that the flight stability at take-off or at landing should, therefore, be evaluated in consideration of the particular aerodynamic characteristics that can be obtained in the accelerating or decelerating time and speed range to be taken.

References

1) Vos, J. B., Rizzi, A., Darracq, D., and Hirschel, E. H.: Navier–Stokes Solvers in European Aircraft Design, *Prog. in Aerospace Sci.*, **24**, 2002, pp. 601-697.
2) Kim, D. H., and Lee, I.: Transonic and Low-Supersonic Aeroelastic Analysis of a Two-Degree-of-Freedom Airfoil with a Freeplay Non-Linearity, *J. Sound and Vibration*, **234** (11), 2000, pp. 859-880.
3) Walsh, J. L., LaMarsh, W. J., and Adelman, H. M.: Fully Integrated Aerodynamic/Dynamic Optimization of Helicopter Rotor Blades, *Mathematical and Computer Modelling*, **18** (3-4), 1993, pp. 53-72.
4) Ahmed, N., Yilbas, B. S., and Budair, M. O.: Computational Study into the Flow Field Developed around a Cascade of NACA 0012 Airfoils, *Comput. Methods in Appl. Mech. and Engrg.*, **167**, 1998, pp. 17-32.
5) Akbari, M. H., and Price, S. J.: Simulation of Dynamic Stall for a NACA 0012 Airfoil Using a Vortex Method, *J. Fluids and Structures*, **17**, 2003, pp. 855-874.
6) Lee, B. H. K.: Self-sustained Shock Oscillations on Airfoils at Transonic Speeds, *Prog. in Aerospace Sci.*, **37**, 2001, pp. 147-196.
7) Mittal, S., and Saxena, P.: Hysteresis in Flow Past a NACA 0012 Airfoil, *Comput. Methods in Appl. Mech. and Engrg.*, **191**, 2002, pp.2179-2189.
8) Ericsson, L. E., and Reding, J. P.: Fluid Dynamic of Unsteady Separated Flow. Part II. Lifting Surfaces, *Prog. in Aerospace Sci.*, **24**, 1987, pp. 249-356.
9) Spalart, P. R., and Allmaras, S. R.: A One Equation Turbulence Model for Aerodynamic Flows, AIAA Paper 92-0439, 1992.
10) Srinivasans, G. R., Ekaterinaris, J. A., and McCroskey, W. J.: Evaluation of Turbulence Models for Unsteady Flows of an Oscillating Airfoil, *Computers & Fluids*, **24** (7), 1995, pp.833-861.